

RESEARCH AND EDUCATION

Impact of 3D resin and base designs on the accuracy of additively manufactured casts using a stereolithography technology

Wenceslao Piedra-Cascón, DDS, MS,^a Carlos Oteo-Morilla, DDS, MS, PhD,^b
Jose Manuel Pose-Rodriguez, DDS, MD, PhD,^c and Mercedes Gallas-Torreira, DDS, PhD^d

Additive manufacturing (AM) is a process where 3-dimensional (3D) objects are manufactured in a layer-by-layer building process.¹⁻³ According to the ASTM F42 Committee, AM technologies are divided in 7 categories: fused deposition modeling (FDM), vat-polymerization or stereolithography (SLA), binder jetting (BJ), material jetting (MJ), sheet lamination, direct energy deposition, and powder-based fusion.^{4,5} SLA technology has gained popularity for fabricating a diverse array of dental devices, including diagnostics casts.⁶ Ultraviolet (UV) light sources used in vat-polymerization 3D printing can be categorized into three types: laser (SLA-Laser), digital light processing (SLA-DLP), and liquid crystal display (SLA-LCD).^{1,7-9}

ABSTRACT

Statement of problem. Three-dimensional (3D) printed casts can be fabricated using a wide range of 3D polymer resins and designed with varying casts' base configurations. Nevertheless, the influence of different base designs, in conjunction with various 3D printing resins, on the final dimensional accuracy of casts manufactured through SLA-LCD 3D printing technology remains unclear.

Purpose. This study assessed the impact of 3D printing resins and base designs on the dimensional accuracy of diagnostic casts fabricated using a SLA-LCD vat-polymerization 3D printer. Two resins (NextDent Model 2.0 and Aqua Gray 4K) and 5 different base configurations were evaluated for their effect on trueness and precision.

Material and methods. A digital maxillary cast was modified into three base designs: solid (Group S), honeycomb (Group HC), and hollow (Group H). Honeycomb and hollow designs had subgroups with 1-mm (HC1, H1) and 2-mm (HC2, H2) wall thicknesses, resulting in 50 specimens (n=10 per subgroup). Eleven embedded precision cubes were used for accuracy assessment. A Sonic Mini 4K vat-polymerization printer was used for cast printing, and dimensional deviations were captured using a coordinate measuring device. Trueness was defined by the average dimensional discrepancy, and precision was indicated by the standard deviation. Statistical analysis included Kruskal-Wallis and Mann-Whitney U tests ($\alpha=.05$).

Results. NextDent resin showed trueness falling between 44.8 μm and 64.5 μm and precision values varying between 33.5 μm and 48.9 μm , while Aqua Gray 4K resin ranged from 24.1 μm to 81.1 μm for trueness and 19.8 μm to 65.9 μm for precision. Significant differences ($P<.001$) were observed in all axes (x-, y-, z-axes) and 3D deviations, influenced by resin and base design.

Conclusions. Resin type and base design significantly affect the dimensional accuracy of 3D printed casts. Aqua Gray 4K with a 2-mm hollow base provided the highest accuracy, particularly when matched with the printer manufacturer. All casts met clinical standards. (J Prosthet Dent xxx;xxx:xxx-xxx)

This research did not receive any specific grant from funding agencies in the public, commercial, or not-for-profit sectors.

The authors declare that they have no known competing financial interests or personal relationships that could have appeared to influence the work reported in this paper.

^aDoctoral student, Doctoral Program in Dental Science, Stomatology Area, Department of Surgery and Medical-Surgery Specialities, University of Santiago de Compostela (USC), Santiago de Compostela, Spain; Affiliate Faculty, Esthetic Dentistry Program, Complutense University of Madrid (UCM), Madrid, Spain; Private practice, Oviedo, Spain; and Researcher, Movumtech, Madrid, Spain.

^bAffiliate Faculty Graduate, Esthetic Dentistry Program, Complutense University of Madrid (UCM), Madrid, Spain; and Private practice, Madrid, Spain.

^cAssociate Lecturer, Adult Comprehensive Dental Clinic, Stomatology Area, Department of Surgery and Medical-Surgery Specialities, Digital Dentistry Unit, School of Dentistry, Faculty of Medicine and Dentistry, University of Santiago de Compostela (USC), Santiago de Compostela, Spain.

^dSenior Lecturer, Planning and Management in Dental Clinics, Stomatology Area, Department of Surgery and Medical-Surgery Specialities, Digital Dentistry Unit, School of Dentistry, Faculty of Medicine and Dentistry, University of Santiago de Compostela (USC), Santiago de Compostela, Spain.

Clinical Implications

The optimal dimensional accuracy of 3D-printed diagnostic casts is attained when the base design is specifically adapted to the chosen resin material. Notably, the same vat-polymerization technology can yield varying levels of accuracy depending on the properties of the 3D polymer resin used.

Multiple variables are known to have an impact on the accuracy of 3D printing, such as the intraoral scanning process,¹⁰ the design's geometries,^{11,12} the resin material,^{13–15} printing technology,^{16,17} the 3D printer,^{16,17} the slicer software program,¹⁸ the print build orientation,^{19,20} the 3D printing parameters,^{3,18,21–27} the support structures,^{11,16,17,28,29,30} and the postprocessing procedures.^{31,32} Furthermore, the accuracy of AM diagnostic casts is influenced by operator choices, namely 3D printer optimal calibration, the holding environment of the polymer material, the ambient temperature, and the digital base 3D designs. Additionally, the digital designer can select among solid, hollow, and honeycomb-based designs. Moreover, dental 3D printer manufacturers do not provide guidelines or recommendations on which wall thicknesses are appropriate in the hollow and honeycomb base designs for fabricating diagnostic casts. However, studies on the impact of different resin materials on additively manufactured diagnostic casts are scarce in the dental literature. Findings from previous studies assessing AM diagnostic casts' accuracy,^{33–38} indicate that possible clinically acceptable manufacturing discrepancies oscillate between 100 μm and 300 μm .^{24,33,35,36}

In accordance with the International Organization for Standardization (ISO) 5725–1 standard, the 3D printer's accuracy is determined by its trueness, which refers to how accurately the 3D printer can reproduce the true form of the digital design specified in the standard tessellation language (STL) file, and precision, that pertains to how consistently the 3D printer performs during the fabrication process under uniform conditions.³⁹

Discrepancies in the accuracy of diagnostic casts produced through 3D printing have been investigated. However, many of these studies still need to consider the manufacturing trinomial concept (MTC),³ encompassing the appropriate combination of printing technology, 3D printer, and polymer material.³ This concept is essential for developing accurate dental 3D printing protocols. Conclusions from studies that overlook the MTC should not be universally generalized as truth. Additional 3D printing research that evaluates accuracy discrepancies within the framework of the MTC is still needed.

This *in vitro* study investigated how 2 different 3D printing polymers affected the diagnostic casts' accuracy using 3 distinct base designs (solid, honeycomb, and hollow) using a 3D printer with SLA-LCD technology (Sonic Mini 4 K; Phrozen). The initial hypothesis was that the 3D printed casts would not differ significantly in accuracy (measured by trueness and precision) across the different base designs when using 2 different resin polymer materials with the same 3D printer.

MATERIAL AND METHODS

A reference standard tessellation language (STL_r) file was generated by digitally scanning a maxillary diagnostic cast with a laboratory scanner (Advaa Lab Scanner; GC). Eleven reference cubes, each measuring 3×3×3 mm, were digitally incorporated into the cast design using an open-source software (Blender 3.3; The Blender Foundation) to enable precise readings (Fig. 1).

Three distinct base designs were developed for the cast: solid (S group), honeycomb (HC group), and hollow (H group). With honeycomb and hollow base designs being further classified into two subgroups according to wall thickness: 1 mm (subgroups HC1 and H1) and 2 mm (subgroups HC2 and H2), resulting in 50 specimens in total, with 10 specimens (n=10) per subgroup.

A single vat-polymerization 3D printer (Sonic Mini 4K; Phrozen) was used to fabricate all specimens with two different resin polymer materials, both compatible with the printer's wavelength: NextDent Model 2.0 (NDM) and Aqua Gray 4K (AG4K) (Table 1). All printing procedures were performed in a dedicated laboratory environment maintained at 23 °C and relative humidity of 50%. Temperature and humidity were monitored continuously using a digital hygrometer/thermometer (Model HT-1; Extech Instruments). The STL files were named according to the resin material and base design: NDM-S, NDM-H1, NDM-H2, NDM-HC1, and NDM-HC2 for the NextDent Model 2.0 group, and AG4K-S, AG4K-H1, AG4K-H2, AG4K-HC1, and AG4K-HC2 for the Aqua Gray 4K group.

All specimens were processed using an open-source slicing tool (Chitubox v1.9.5; Chitubox) (Fig. 2A, B). Each specimen was oriented horizontally on the build platform (0-degree angle) at a layer thickness of 50- μm , along with the same support structures for both resins (Fig. 2C, D). NextDent Model 2.0 resin was mixed for 2.5 hours, while Aqua Gray 4K was mixed for 5 minutes following manufacturers recommendations, using an oscillatory mixer (LC-3D Mixer; 3D Systems) to ensure homogeneity of the material. Manufacturer's recommendations were followed to calibrate the SLA-LCD Sonic Mini 4K 3D printer (Phrozen3D), with an XY resolution of 35 μm and a wavelength of 405 nm.

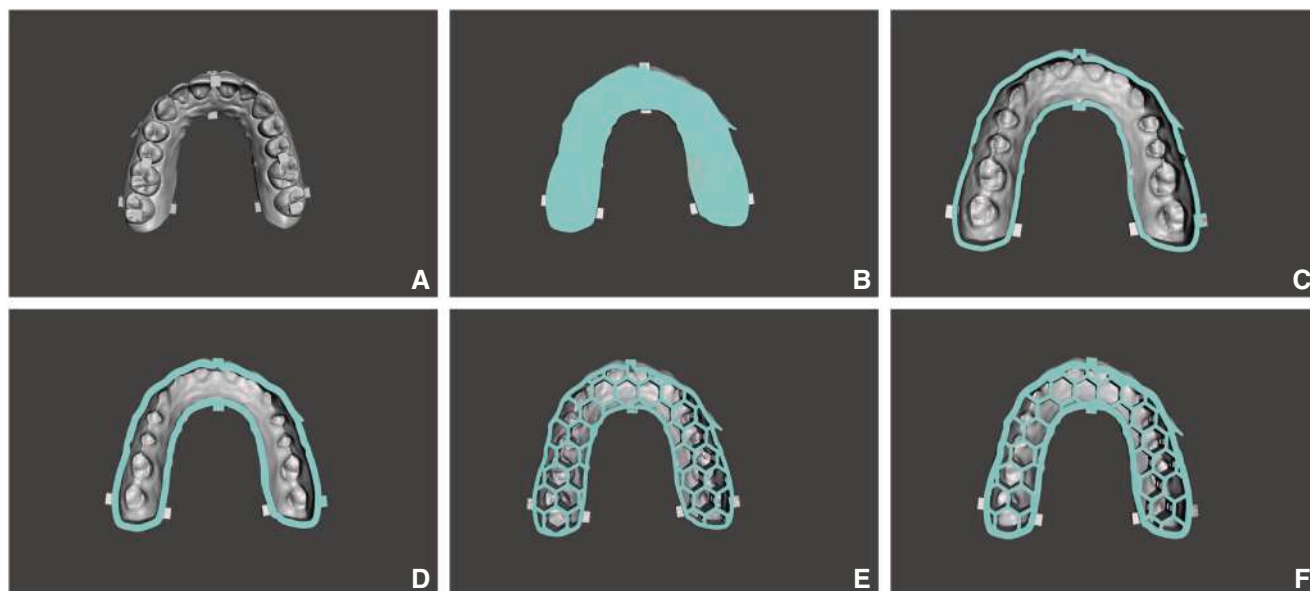


Figure 1. Digital design of maxillary virtual diagnostic cast of each group. A, Occlusal view. B, Solid. C, 1-mm wall thickness hollow, D, 2-mm wall thickness hollow, E, 1-mm wall thickness honeycomb, F, 2-mm wall thickness honeycomb.

Table 1. Specifications of polymer resin materials

Brand	Resin	Wavelength	Hardness	Flexural Modulus
NextDent	Model 2.0 Gray	405 nm	≥ 80 shore D	≥1500 MPa
Phrozen	Aqua Gray 4K	405 nm	80 shore D	1260–1520 MPa

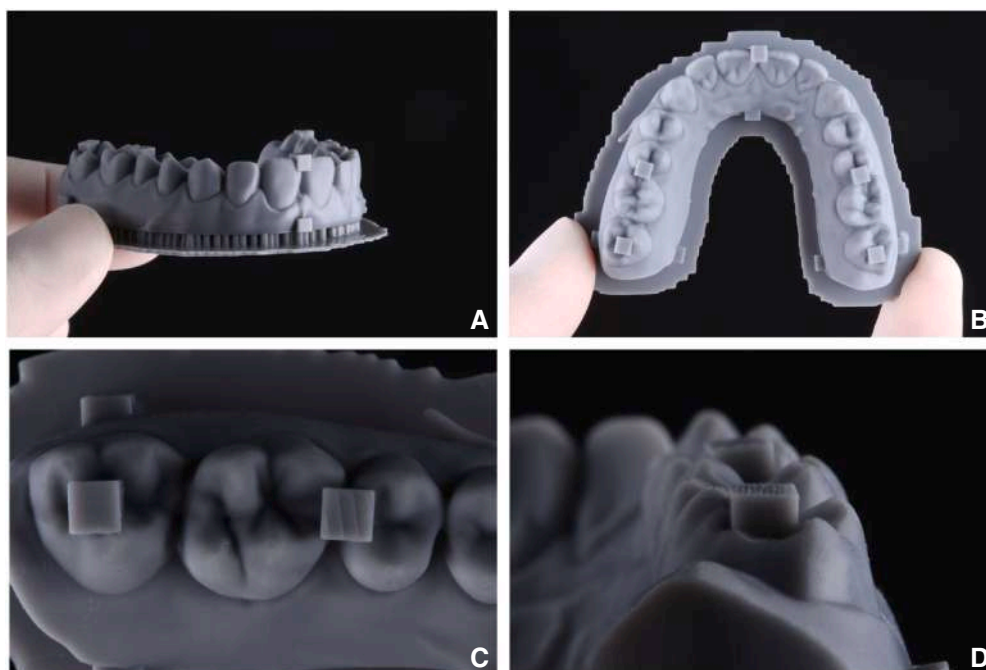


Figure 2. Additive manufactured diagnostic cast with reference cubes. A, Support structures. B, Global occlusal view. C, Sextant occlusal view. D, Lateral view.

Once printed, a spatula was used to remove the specimens from the build platform (iFixit; iFixit GmbH), which were subjected to a two-step cleaning process.

First, the specimens were placed in an ultrasonic bath containing 99% isopropyl alcohol (IPA) (IPA 99%; EQM Soluciones Químicas) for 3 minutes, with a second

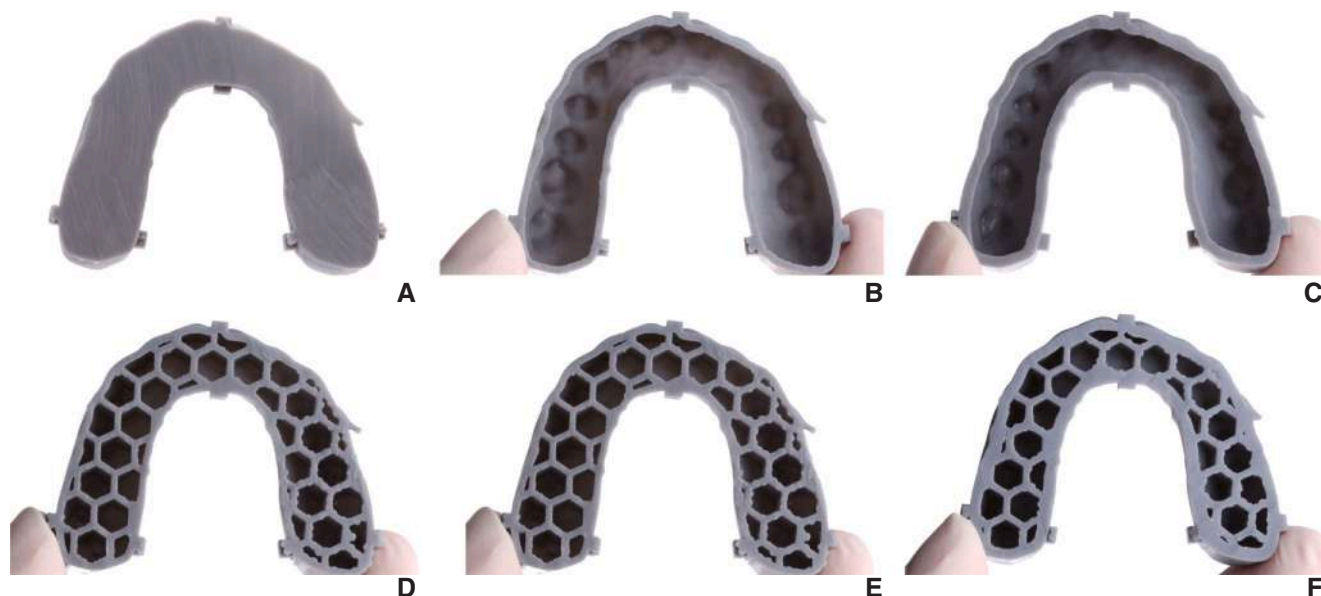


Figure 3. Additive manufacturing digital diagnostic cast base design for each group. A, Solid. B, 1-mm wall thickness hollow, C, 2-mm wall thickness hollow, D, 1-mm wall thickness honeycomb, E, 2-mm wall thickness honeycomb.

ultrasonic bath in fresh IPA for another 2 minutes. After being dried with compressed air, they were left at room temperature in a dark environment for 15 minutes to allow complete evaporation of the alcohol. A UV polymerization chamber was used to perform post-curing: 10 minutes for the NextDent Model 2.0 specimens and 6 minutes for the Aqua Gray 4K specimens, using the manufacturer-recommended curing devices (LC-3D Print Box; 3D Systems for NextDent, and Curing Station; Phrozen for Aqua Gray 4K). 50 specimens were successfully fabricated in total (Fig. 3).

Dimensional accuracy was measured using a coordinate measuring machine (CMM) (DEA Alpha Status; Hexagon AB). To assess accuracy, the X, Y, and Z coordinates of the 11 embedded cubes (each 3×3×3 mm) were measured, supplemented by 36 additional points

on the cast surface (Table 2). A measurement program was developed using the CAD casts of the different cast base designs to automate the evaluation process. Upon receiving the printed specimens, each was securely fixed within the CMM's measurement volume. The measurement sequence began with an alignment of the physical specimen to its corresponding CAD cast. For alignment, 13 reference points were defined in the CAD, one at the geometric center of each fully intact cube face. These central points were palpated on the physical specimen using the CMM, with the stylus contacting the midpoint of each selected face to establish spatial correspondence between the digital and printed casts.

The coordinate system's origin (0, 0, 0) was defined in the CAD cast as the centroid of the maxillary cast, located at the intersection of the midsagittal plane and the

Table 2. Description of 36 additional points measured on additively manufactured specimens with coordinate measurement machine

Additional Point	Location
Dental 1	Tip of distobuccal cusp of right and left first molars
Dental 2	Tip of distobuccal cusp of right and left second molars
Dental 3	Tip of mesiolingual cusp of right and left first molars
Dental 4	Tip of mesiolingual cusp of right and left second molars
Dental 5	Tip of buccal cusp of right and left first premolars
Dental 6	Tip of lingual cusp of right and left first premolars
Dental 7	Tip of cusp of right and left canines
Dental 8	Distobuccal edge of right and left lateral incisors
Dental 9	Mesiobuccal edge of right and left lateral incisors
Dental 10	Distobuccal edge of right and left central incisors
Gingival Buccal 1	5 mm apically to buccal interdental papilla between right and left second and first molars on both right and left sides
Gingival Buccal 2	5 mm apically to buccal interdental papilla between first molar and second premolar on both right and left sides
Gingival Buccal 3	5 mm apically to buccal interdental papilla between first premolar and canine on both right and left sides
Gingival Buccal 4	5 mm apically to buccal interdental papilla between lateral and central incisors on both right and left sides
Gingival Palatal 1	5 mm apically to palatal interdental papilla between second and first molars on both right and left sides
Gingival Palatal 2	5 mm apically to palatal interdental papilla between first molar and second premolar on both right and left sides
Gingival Palatal 3	5 mm apically to palatal interdental papilla between first premolar and canine on both right and left sides
Gingival Palatal 4	5 mm apically to palatal interdental papilla between right and left central incisors

transverse plane. This reference point was consistently applied during CMM measurements to ensure alignment accuracy. Following initial alignment, the predefined measurement program automatically recorded the X, Y, and Z coordinates of all specified points (11 cube centers and 36 additional surface points) on the specimen. Each point was measured once, leveraging the CMM's to ensure reliable data.

The STL file of the digital cast was converted into a CAD cast using a software program (Metrolog X4 v18; Metrologic Group), as the CMM requires a solid surface cast rather than a mesh for accurate evaluation. Following measurement, a best-fit adjustment was performed using the eleven reference cubes to align the measured data with the CAD cast, using a local best-fit algorithm. This optimization minimized deviations between the digital and printed casts, enabling the calculation of absolute dimensional differences between the CAD design and the physical specimens.

In this experiment, trueness was determined by the average of the absolute dimensional differences between the digital and printed casts, while precision was

characterized by the standard deviation of these differences. Statistical analysis was conducted through a Kruskal-Wallis test for independent samples, subsequently using the Mann-Whitney U pairwise comparisons ($\alpha=.05$), using a statistical software program (IBM SPSS Statistics, v25; IBM Corp).

RESULTS

Table 3 shows the median values along with the \pm interquartile range (IQR) for all axes (x-, y- and z-), along with 3D discrepancies. Table 4 presents the resulting trueness and precision. The 5 digital cast base designs were significantly different in the x-, y-, and z-axes and the 3D discrepancy as indicated by the Kruskal-Wallis' test for independent samples (all $P<.001$) independently of the 3D printer used. The Mann-Whitney U pairwise comparison test for independent samples identified significant differences between the AG4K and NDM resin groups in the x-, y-, and z-axes and in the 3D discrepancy (all $P<.001$), regardless of which cast base design was used (Table 4).

Table 3. Median dimensional discrepancies with interquartile ranges (IQR) of additively manufactured casts across different resin materials and base designs (μm)

Discrepancy Measurement	Resin Material	Group	Median \pm Interquartile Range	Percentile 25	Percentile 75	
x-axis	NDM	H1	26.90 \pm 66.60	8.10	58.50	
		H2	18.80 \pm 41.0	6.00	35.00	
		HC1	24.40 \pm 56.70	7.60	49.10	
		HC2	23.90 \pm 54.80	5.70	49.10	
		S	26.60 \pm 73.70	9.00	64.70	
	AG4K	H1	11.80 \pm 34.50	3.70	30.80	
		H2	8.20 \pm 20.50	3.10	17.40	
		HC1	35.10 \pm 84.30	12.90	71.40	
		HC2	13.80 \pm 38.00	4.60	33.40	
		S	20.00 \pm 66.00	6.80	59.20	
	y-axis	NDM	H1	14.60 \pm 35.70	6.70	29.00
			H2	8.70 \pm 24.50	2.80	21.70
			HC1	11.20 \pm 27.70	4.30	23.40
			HC2	11.80 \pm 28.00	4.60	23.40
			S	15.60 \pm 37.90	6.50	31.40
AG4K		H1	7.90 \pm 21.50	2.50	19.00	
		H2	4.80 \pm 14.40	1.30	13.10	
		HC1	14.2 \pm 37.50	5.20	32.30	
		HC2	7.60 \pm 19.40	3.30	16.10	
		S	14.40 \pm 32.20	4.20	28.00	
z-axis	NDM	H1	28.10 \pm 67.60	13.30	54.30	
		H2	22.20 \pm 47.00	9.50	37.50	
		HC1	25.10 \pm 56.7	12.00	44.70	
		HC2	22.80 \pm 48.30	9.30	39.00	
		S	29.50 \pm 65.10	14.50	50.60	
	AG4K	H1	16.90 \pm 39.50	4.60	34.90	
		H2	9.90 \pm 22.50	4.60	17.90	
		HC1	31.20 \pm 76.70	16.80	59.90	
		HC2	12.60 \pm 38.90	4.10	34.80	
		S	24.00 \pm 58.50	8.40	50.10	
	3D Discrepancy	NDM	H1	52.50 \pm 11.31	26.50	86.60
			H2	36.80 \pm 81.20	19.30	61.90
			HC1	45.40 \pm 98.40	21.20	77.20
			HC2	45.20 \pm 90.20	21.20	69.00
			S	55.80 \pm 123.00	30.80	92.20
AG4K		H1	29.20 \pm 68.70	11.40	57.30	
		H2	19.40 \pm 43.60	9.20	34.40	
		HC1	61.70 \pm 148.90	32.70	116.20	
		HC2	25.90 \pm 66.60	12.50	54.10	
		S	49.40 \pm 105.80	20.20	85.60	

Table 4. Trueness and precision values obtained for different groups tested (μm)

	Resin Material	Group	Trueness	Precision
x-axis	NDM	H1	41.20	44.40
		H2	27.10	28.20
		HC1	31.70	28.20
		HC2	33.40	34.20
		S	39.10	36.10
	AG4K	H1	22.50	26.90
		H2	12.50	13.40
		HC1	48.00	45.70
		HC2	23.60	27.50
		S	35.10	36.10
y-axis	NDM	H1	21.00	20.60
		H2	14.20	15.10
		HC1	16.90	18.60
		HC2	16.30	15.20
		H1	23.30	23.50
	AG4K	H2	14.10	18.00
		HC1	10.40	14.40
		HC2	27.80	40.40
		S	11.90	13.10
		S	20.00	20.40
z-axis	NDM	H1	35.70	27.20
		H2	26.40	21.50
		HC1	32.20	27.40
		HC2	26.50	20.70
		S	35.00	25.70
	AG4K	H1	24.00	26.30
		H2	13.10	12.20
		HC1	46.10	44.60
		HC2	23.60	26.60
		S	32.60	29.10
3D Discrepancy	NDM	H1	64.50	48.90
		H2	44.80	33.50
		HC1	52.50	38.30
		HC2	50.40	37.10
		S	64.20	41.20
	AG4K	H1	39.80	37.90
		H2	24.10	19.80
		HC1	81.10	65.90
		HC2	39.00	37.00
		S	57.50	44.20

Considering the 3D printer, polymer resin materials, and cast base design, the following results were obtained in the x-, y-, and z-axes and the 3D discrepancy. For the x-axis discrepancy, the Mann-Whitney U pairwise comparison test for independent samples revealed significant differences between NDM-H1 ($26.9 \pm 66.6 \mu\text{m}$) and AG4K-H1 ($11.8 \pm 34.5 \mu\text{m}$) ($P < .001$), NDM-H2 ($18.8 \pm 41 \mu\text{m}$) and AG4K-H2 ($8.2 \pm 20.5 \mu\text{m}$) ($P < .001$), NDM-HC1 ($24.4 \pm 56.7 \mu\text{m}$) and AG4K-HC1 ($35.1 \pm 84.3 \mu\text{m}$) ($P < .001$), and NDM-HC2 ($23.9 \pm 54.8 \mu\text{m}$) and AG4K-HC2 ($13.8 \pm 38 \mu\text{m}$) ($P < .001$) but not for NDM-S ($26.6 \pm 73.7 \mu\text{m}$) and AG4K-S ($20 \pm 66 \mu\text{m}$) ($P = .549$) (Fig. 4A). For the y-axis analysis using the Mann-Whitney U pairwise comparison test, significant differences were detected between NDM-H1 ($14.6 \pm 35.7 \mu\text{m}$) and AG4K-H1 ($7.9 \pm 21.5 \mu\text{m}$) ($P < .001$), NDM-H2 ($8.7 \pm 24.5 \mu\text{m}$) and AG4K-H2 ($4.8 \pm 14.4 \mu\text{m}$) ($P < .001$), NDM-HC1 ($11.2 \pm 27.7 \mu\text{m}$) and AG4K-HC1 ($14.2 \pm 37.5 \mu\text{m}$) ($P < .005$), and NDM-HC2 ($11.8 \pm 28 \mu\text{m}$) and AG4K-HC2 ($7.6 \pm 19.4 \mu\text{m}$) ($P < .000$) but not for NDM-S ($15.6 \pm 37.9 \mu\text{m}$) and AG4K-S ($14.4 \pm 32.2 \mu\text{m}$) ($P > .999$) (Fig. 4B). In the case of the z-axis analysis using the Mann-Whitney U pairwise comparison test, significant differences were revealed between NDM-H1

($28.1 \pm 67.6 \mu\text{m}$) and AG4K-H1 ($16.9 \pm 39.5 \mu\text{m}$) ($P < .001$), NDM-H2 ($22.2 \pm 47 \mu\text{m}$) and AG4K-H2 ($9.9 \pm 22.5 \mu\text{m}$) ($P < .001$), NDM-HC1 ($25.1 \pm 56.7 \mu\text{m}$) and AG4K-HC1 ($31.2 \pm 76.7 \mu\text{m}$) ($P < .001$), and NDM-HC2 ($22.8 \pm 48.3 \mu\text{m}$) and AG4K-HC2 ($12.6 \pm 38.9 \mu\text{m}$) ($P < .001$) but not for NDM-S ($29.5 \pm 65.1 \mu\text{m}$) and AG4K-S ($24 \pm 58.5 \mu\text{m}$) ($P = .222$) (Fig. 4C). Finally, the analysis of 3D discrepancy using the Mann-Whitney U pairwise comparison test highlighted significant differences between NDM-H1 ($52.5 \pm 113.1 \mu\text{m}$) and AG4K-H1 ($29.2 \pm 68.7 \mu\text{m}$) ($P < .001$), NDM-H2 ($36.8 \pm 81.2 \mu\text{m}$) and AG4K-H2 ($19.4 \pm 43.6 \mu\text{m}$) ($P < .001$), NDM-HC1 ($45.4 \pm 98.4 \mu\text{m}$) and AG4K-HC1 ($61.7 \pm 148.9 \mu\text{m}$) ($P < .001$), and NDM-HC2 ($45.2 \pm 90.2 \mu\text{m}$) and AG4K-HC2 ($25.9 \pm 66.6 \mu\text{m}$) ($P < .001$) but not for NDM-S ($55.8 \pm 123 \mu\text{m}$) and AG4K-S ($49.4 \pm 105.8 \mu\text{m}$) ($P = .061$) (Fig. 4D).

DISCUSSION

According to these findings, there was substantial variation in trueness and precision across the x-, y-, and z-axes, as well as 3D discrepancy between the tested groups. However, only the 3D discrepancy for solid cast

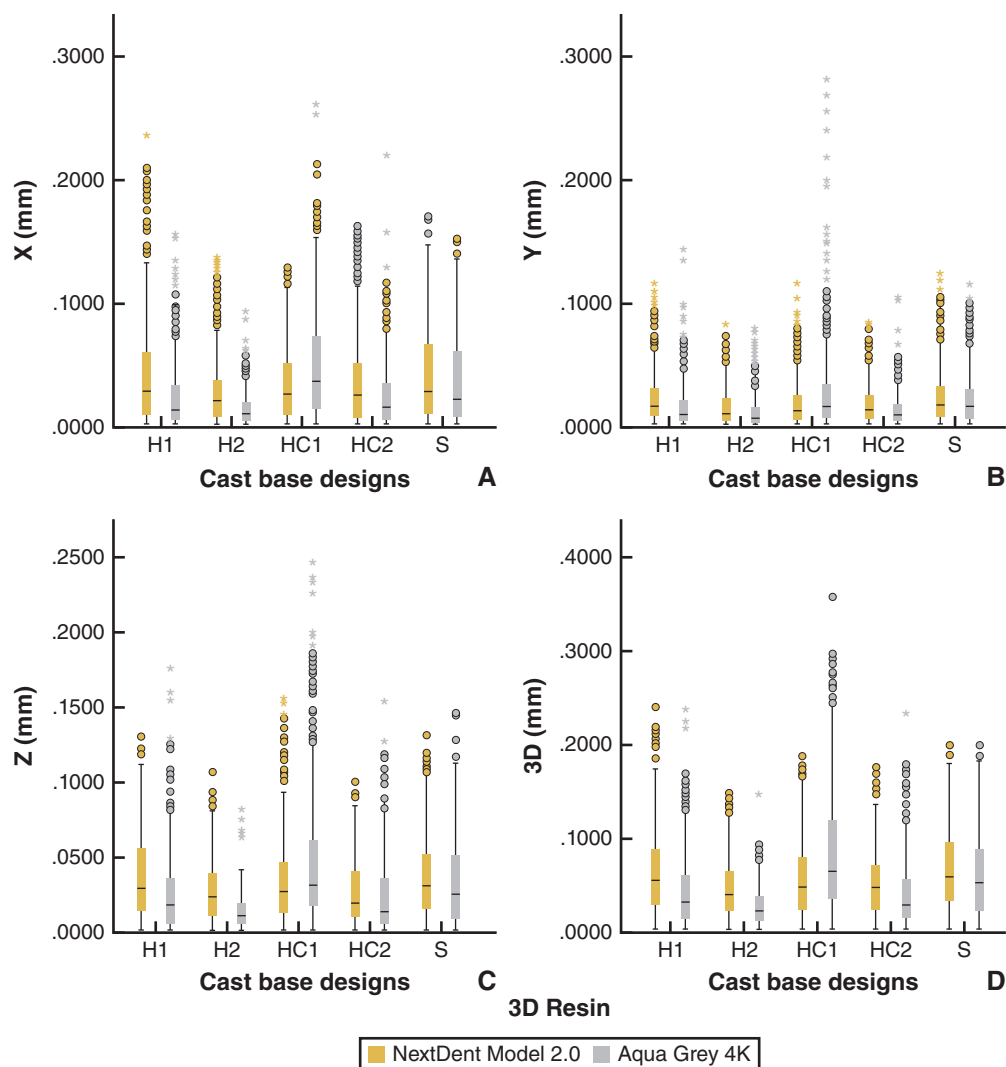


Figure 4. Measured discrepancies of material polymer groups tested. A, x-axis. B, y-axis. C, z-axis. D, 3D discrepancy.

base designs produced with NexDent Model 2.0 or Aqua Gray 4K resins were statistically similar. Consequently, the null hypothesis that accuracy (trueness and precision) would not vary significantly among the different base designs when using the same vat-polymerization technology and 2 different resin polymer materials was rejected. The findings revealed that the Aqua Gray 4K resin group achieved the highest manufacturing accuracy with a hollow base design featuring a 2-mm wall thickness, registering a trueness of 24.1 μm and a precision of 19.8 μm . Likewise, the NexDent Model 2.0 group attained optimal accuracy using the same hollow 2-mm wall thickness design, with a trueness of 44.8 μm and a precision of 33.5 μm .

The present in vitro study showed manufacturing trueness across the tested groups ranging from 24.1 μm to 81.1 μm , while precision oscillated between 19.8 μm and 65.9 μm , all within clinically acceptable limits. Despite the variety of clinical and laboratory conditions,

these levels of manufacturing accuracy should not hinder the application of 3D printed casts in the production of thermoplastic devices or silicone indexes. Moreover, the accuracy observed in both 3D printing devices suggests they could be suitable for creating definitive casts, although this conclusion warrants further investigation, as the effectiveness of printed casts in permanent restorations depends on both dimensional accuracy and surface quality.

Calibration of the 3D printing device in this study was performed as indicated by the manufacturer's guidelines using 2 polymer resin materials (NextDent Model 2.0; 3D Systems and Aqua Gray 4K; Phrozen) and the same support structures. The printing process was conducted by a clinician (W.P.C.) with 7 years of experience in 3D printing. For postprocessing procedures, casts printed with NexDent Model 2.0 resin were polymerized with the recommended UV device (LC-3DPrint Box; 3D Systems), and casts printed using Aqua Gray 4K resin employed the

Phrozen polymerization machine (Curing Station; Phrozen) to obtain the optimal properties of the resins according to the manufacturer's recommendations. To the knowledge of the authors, this is the first *in vitro* study that employs the same 3D printing device and 2 different resin materials to validate the manufacturing trinomial and demonstrate that the same 3D printer can yield different accuracies depending on the resin polymer material used. The accuracy of 3D printed casts has been analyzed in previous studies, registering trueness values between 21.83 μm and 289 μm and precision values spanning from 17.82 μm to 284 μm . However, most studies compared different 3D printers and different resin polymer materials. Thus, a comprehensive comparison of data between different 3D printing systems is impossible. Also, none of the previous studies reported the cast base design selected. The impact that the cast base designs have on the manufacturing accuracy of 3D printing diagnostic casts has been studied.^{34,37,40} Rungrojwittayakul et al³⁴ analyzed the differences between two different base designs (solid and hollow) fabricated with 2 distinct vat-polymerization technologies, SLA-DLP/CLIP (Carbon M2; Carbon) and SLA-DLP (MoonRay S100; Sprintray), reporting that the highest accuracy was achieved using solid base designs, with trueness values between 48 μm and 87 μm and precision values that ranged from 44 μm to 57 μm . Chen et al³⁵ evaluated two different 3D printing technologies: an SLA-Laser 3D printer (Form 3; Formlabs) and a DLP 3D printer (Straumann P30+; Rapidshape). Each printer was tested with a different resin polymer material: Model Resin V3 (Formlabs) for the Form 3 and P Pro Master Model (Institut Straumann AG) for the Straumann P30+. After printing, all casts were post-cured using the manufacturer-recommended curing machine for each 3D printer, reporting that casts with a hollow interior without a base (HB) exhibited significantly lower trueness (Form 3: 94.06 \pm 3.43 μm ; Straumann P30+: 114.03 \pm 2.75 μm) and precision (Form 3: 66.65 \pm 3.06 μm ; Straumann P30+: 29.78 \pm 1.90 μm) than designs with a base, such as hollow with perforated base (HWB) (Form 3: trueness 70.61 \pm 2.15 μm , precision 46.06 \pm 3.31 μm ; Straumann P30+: trueness 98.06 \pm 2.20 μm , precision 24.38 \pm 2.36 μm) or solid (S) (Form 3: trueness 85.28 \pm 2.49 μm , precision 42.63 \pm 4.09 μm ; Straumann P30+: trueness 98.01 \pm 4.95 μm , precision 20.96 \pm 0.95 μm). Their study underscores the necessity of a base for maintaining accuracy, attributing the HB design's inferior performance to insufficient structural support during layer-by-layer polymerization. While our study did not test a baseless design, the superior accuracy of the hollow base (H2) over solid and honeycomb configurations echoes Chen et al³⁵ finding that a base enhances stability, though our results further indicate that hollowing with an optimal wall thickness (2 mm) outperforms a solid structure in

trueness, possibly due to reduced material-related distortions in the SLA-LCD process. These differences may also reflect the interplay between resin properties and printer technology, reinforcing the manufacturing trinomial concept's relevance in optimizing 3D printing outcomes. Moreover, differences in print orientations, layer thicknesses, support structures, manufacturing trinomial, 3D printer technologies, resin polymer materials and measurement approaches, make it challenging to compare previous investigations with the results presented here. Revilla-León et al³⁷ studied the same cast base designs as in the present study. They tested solid, honeycomb, and hollow casts with base designs featuring wall thicknesses of 1 mm and 2 mm using an SLA-DLP 3D printer (NextDent 5100; 3D Systems) and NextDent Model resin polymer material. They concluded that solid casts showed the highest accuracy values at 63.73 \pm 45.42 μm . Piedra-Cascón et al⁴⁰ studied the impact of the same base designs used by Revilla-León et al³⁷ but using two 3D printers, an SLA-DLP (NextDent 5100; 3D Systems) and Sonic Mini 4K; Phrozen) with an identical polymer material (NextDent Model 2.0). The authors reported the best manufacturing accuracy for the NextDent 3D printer to be 21.83 \pm 18.4 μm . The possible reason for different manufacturing accuracies using the same 3D printer and polymer material could be that their study involved fabricating the specimens vertically in contrast with Piedra-Cascón et al,⁴¹ where all the specimens were 3D printed horizontally; this could have influenced the final results. When a diagnostic cast is fabricated in a vertical orientation, it is probable that the increased hollowness leaves the walls unsupported, potentially leading to distortions. Piedra-Cascón et al⁴¹ also reported that the Phrozen Sonic Mini 4K 3D printer, when paired with NextDent Model 2.0 polymer material, achieved its highest manufacturing accuracy with a trueness of 45.15 \pm 33.51 μm using a 2-mm hollow cast base design and printed horizontally. They reported statistically significant differences between Sonic Mini 4K and NextDent 5100 3D printers when the same NextDent Model 2.0 polymer material was used, with the NextDent 5100 3D printer being better than the Sonic Mini 4K. The study presented here aimed to provide insights into the accuracy of the Sonic Mini 4K printer using 2 different resins (NextDent Model 2.0; NextDent and Aqua Gray 4K; Phrozen). Using the same dataset as in previous studies,^{37,40} the results revealed that the combination of Phrozen's 3D printer and resin achieved an accuracy of 24.1 \pm 19.8 μm similar to the results obtained using NextDent's 3D printing workflow.⁴⁰ These results show that not all resins can achieve the same level of accuracy even when their wavelength is compatible with the printer. This reinforces the need to understand the manufacturing trinomial concept applied to the 3D printing system used.³

Various approaches have been used to evaluate the accuracy of 3D printed casts produced with SLA technologies, including manual measurements using digital calipers, as well as digital techniques involving superimposition to obtain linear and angular measurements, often using root mean square (RMS) values.^{20,39} Nevertheless, a coordinate measuring machine (CMM) is typically employed to perform such measurements.³⁸

SLA 3D printers can be divided into open and closed systems, with the first providing flexibility in the customization of printing parameters and their interrelation with printing zones. In theory, when the wavelengths of polymer materials and 3D printing devices are compatible, they can be used interchangeably. Maneiro-Lojo et al²⁰ reported manufacturing accuracy ranging from 92 to 131 μm with an open-source SLA-LCD printer (Photon Mono SE; Anycubic) when using Aqua Gray 4K polymer material. In contrast, the current study found that the Sonic Mini 4K paired with the same Aqua Gray 4K resin achieved a manufacturing accuracy between 4.3 and 43.9 μm . The discrepancies between these studies could stem from differences in cast base designs, settings of the support structure, printing parameters, and postprocessing procedures. However, this investigation indicates that even when the wavelength of the resin materials and the 3D printer's UV light source are compatible, changes in accuracy are likely associated with the need for adjustments within the manufacturing trinomial concept.³ Differences in accuracy between the two 3D polymer resin materials tested may also be attributed to differences in their formulations, including the types of photo-initiators used and the presence or absence of anti-sedimentation technology.

One of the main limitations of this study is the fact that only one 3D printer was tested with 2 resin polymer materials. Further research is necessary to investigate the manufacturing process using different 3D printing systems. This will help optimize the 3D printing workflow's accuracy, making it suitable for more complex applications.

CONCLUSIONS

Based on the findings of this in vitro study, the following conclusions were drawn:

1. The type of material polymer had an impact on the manufacturing accuracy with the same 3D printing technology.
2. The 2-mm wall thickness hollow design displayed the highest accuracy in casts produced using an SLA-LCD technology with Aqua Gray 4K resin material.
3. The highest manufacturing accuracy for Aqua Gray 4K specimens ranged from 4.3 to 43.9 μm .
4. The digital base designs impacted the manufacturing accuracy of the fabricated casts.

5. Solid casts were the least influenced by the printer/resin combination.

REFERENCES

1. Hull C.W. Apparatus for production of three-dimensional objects by stereolithography 1986, US Patent 4575330.
2. Glossary of Digital Dental Terms, 2nd Edition: American College of Prosthodontists and ACP Education Foundation. *J Prosthodont.* 2021;30:172–181.
3. Piedra-Cascón W, Krishnamurthy VR, Att W, Revilla-León M. 3D printing parameters, supporting structures, slicing, and postprocessing procedures of vat-polymerization additive manufacturing technologies: A narrative review. *J Dent.* 2021;109:10363.
4. ISO 17296-2:2015. Additive manufacturing general principles part 2: overview of process categories and feedstock. Last Accessed 01/08/2024.
5. ASTM, Committee F42 on Additive Manufacturing Technologies, West Conshohocken, Pa. 2009 Standard terminology for additive manufacturing general principles and terminology. ISO/ASTM52900-15. Last Accessed 01/08/2024.
6. Revilla-León M, Özcan M. Additive manufacturing technologies used for processing polymers: Current status and potential application in prosthetic dentistry. *J Prosthodont.* 2019;28:146–158.
7. Hornbeck L. Digital micromirror device 2009. US Patent No. 5061.049.
8. ISO 17296e2. Additive manufacturing general principles part 2: Overview of process categories and feedstock. 2015. Available at: <https://www.iso.org/standard/61626.html?browse=tc>.
9. Holt P.M. Maskless photopolymer exposure process and apparatus 2012. US Patent 8.114.569 B2.
10. Piedra-Cascón W, Adhikari RR, Özcan M, et al. Accuracy assessment (trueness and precision) of a confocal based intraoral scanner under twelve different ambient lighting conditions. *J Dent.* 2023;134:104530.
11. Ide Y, Nayar S, Logan H, et al. The effect of the angle of acuteness of additive manufactured models and the direction of printing on the dimensional fidelity: Clinical implications. *Odontology.* 2017;105. 108e115.
12. Wu D, Zhao Z, Zhang Q, et al. Mechanics of shape distortion of DLP 3D printed structures during UV post-curing. *Soft Matter.* 2019;15:6151–6159.
13. Alharbi N, Osman R, Wismeijer D. Effect of build direction on the mechanical properties of 3D printed complete coverage interim dental restorations. *J Prosthet Dent.* 2016;155:760–767.
14. Reymus M, Fabritius R, Kebler A, et al. Fracture load of 3D-printed fixed dental prostheses compared with milled and conventionally fabricated ones: The impact of resin material, build orientation, postcuring and artificial aging: An in vitro study. *Clin Oral Investig.* 2020;24:701–710.
15. Revilla-León M, Umorin M, Özcan M, Piedra-Cascón W. Color dimensions of additive manufactured interim restorative dental material. *J Prosthet Dent.* 2020;123:754–760.
16. Puebla K, Arcaute K, Quintana R, Wicker RB. Effects of environmental conditions, aging, and build orientations on the mechanical properties of ASTM type I specimens manufactured via stereolithography. *Rapid Prototyp J.* 2012;18:374–388.
17. Braian M, Jimbo R, Wennerberg A. Production tolerance of additive manufactured polymeric objects for clinical applications. *Dent Mater.* 2016;32:853–861.
18. Arnold C, Monsees D, Hey J, Schweyen R. Surface quality of 3D-printed models as a function of various printing parameters. *Materials (Basel).* 2019;12:19.
19. Revilla-León M, Jordan D, Methani MM, et al. Influence of printing angulation on the surface roughness of additive manufactured clear silicone indices: An in vitro study. *J Prosthet Dent.* 2021;125:462–468.
20. Maneiro Lojo J, Alonso Pérez-Barquero J, García-Sala Bonmatí F, et al. Influence of print orientation on the accuracy (trueness and precision) of diagnostic casts manufactured with a daylight polymer printer. *J Prosthet Dent.* 2024;132:1314–1322.
21. Park GS, Kim SK, Heo SJ, et al. Effects of printing parameters on the fit of implant-supported 3D printing resin prosthetics. *Materials (Basel).* 2019;12:2533.
22. Zhang ZC, Li PL, Chu FT, Shen G. Influence of the three-dimensional printing technique and printing layer thickness on model accuracy. *J Orofac Orthop.* 2019;80:194–204.
23. Loflin WA, English JD, Borders C, et al. Effect of print layer height on the assessment of 3D-printed models. *Am J Orthod Dentofacial Orthop.* 2019;156:283–289.
24. Favero CS, English JD, Cozad BE, et al. Effect of print layer height and printer type on the accuracy of 3-dimensional printed orthodontic models. *Am J Orthod Dentofacial Orthop.* 2017;152:557–565.
25. Reymus M, Lümekemann N, Stawarczyk B. 3D printed material for temporary restorations: Impact of print layer thickness and post-curing method on degree of conversion. *Int J Comput Dent.* 2019;22:231–237.

26. Chockalingam K, Jawahar N, Chandrasekhar U. Influence of layer thickness on mechanical properties in stereolithography. *Rapid Prototyp J*. 2006;12:106–113.
27. Scherer M, Al-Haj Husain N, Barmak AB, et al. Influence of the layer thickness on the flexural strength of aged and nonaged additively manufactured interim dental material. *J Prosthodont*. 2023;32:68–73.
28. Cho HS, Park WS, Choi BW, Leu MC. Determining optimal parameters for stereolithography processes via genetic algorithm. *J Manuf Syst*. 2000;19:18–27.
29. Alharbi N, Osman RB, Wismeijer D. Factors influencing the dimensional accuracy of 3D-printed full-coverage dental restorations using stereolithography technology. *Int J Prosthodont*. 2016;29:503–510.
30. Unkovskiy A, Bui PH, Schille C, et al. Objects build orientation, positioning, and curing influence dimensional accuracy and flexural properties of stereolithographically printed resin. *Dent Mater*. 2018;34:324–333.
31. Mostafavi D, Methani MM, Piedra-Cascón W, et al. Influence of the rinsing postprocessing procedures on the manufacturing accuracy of vat-polymerized dental model material. *J Prosthodont*. 2021;30:610–616.
32. Mostafavi D, Methani MM, Piedra-Cascón W, et al. Influence of polymerization postprocessing procedures on the accuracy of additively manufactured dental model material. *Int J Prosthodont*. 2023;36:479–485.
33. Etemad-Shahidi Y, Qallandar OB, Evenden J, et al. Accuracy of 3-dimensionally printed full-arch dental models: A systematic review. *J Clin Med*. 2020;9:3357.
34. Rungrojwittayakul O, Kan JY, Shiozaki K, et al. Accuracy of 3D printed models created by two technologies of printers with different designs of model base. *J Prosthodont*. 2020;29:124–128.
35. Chen Y, Li H, Zhai Z, et al. Impact of internal design on the accuracy of 3-dimensionally printed casts fabricated by stereolithography and digital light processing technology. *J Prosthet Dent*. 2023;130:381.e1–381.e7.
36. Kim SY, Shin YS, Jung HD, et al. Precision and trueness of dental models manufactured with different 3-dimensional printing techniques. *Am J Orthod Dentofacial Orthop*. 2018;153:144–153.
37. Dietrich CA, Ender A, Baumgartner S, Mehl A. A validation study of reconstructed rapid prototyping models produced by two technologies. *Angle Orthod*. 2017;87:782–787.
38. Revilla-León M, Piedra-Cascón W, Aragonese R, et al. Influence of base design on the manufacturing accuracy of vat-polymerized diagnostic casts: An in vitro study. *J Prosthet Dent*. 2023;129:166–173.
39. Morón-Conejo B, López-Vilagrán J, Cáceres D, et al. Accuracy of five different 3D printing workflows for dental models comparing industrial and dental desktop printers. *Clin Oral Investig*. 2023;27:2521–2532.
40. ISO 5725–1. Accuracy (trueness and precision) of measuring methods and results. Part-1: General principles and definitions.
41. Piedra-Cascón W, Pérez-López J, Veiga-López B, et al. Influence of base designs on the manufacturing accuracy of vat-polymerized diagnostic casts using two different technologies. *J Prosthet Dent*. 2024;132:453.e1–453.e9.

Corresponding author:

Dr Wenceslao Piedra-Cascón
Rúa Entrerriós s/n
Santiago de Compostela 15782
SPAIN.
Email: wpiedra@movumtech.com

Acknowledgments

The authors thank Dental Astur dental laboratories for their support with NextDent technologies.

CRediT authorship contribution statement

Wenceslao Piedra-Cascón: Idea, conceptualization, protocol development, results interpretation, Phrozen manufacturing procedures and contributed to the manuscript writing. **Carlos Oteo-Morilla:** Statistical analysis and contributed to the manuscript writing. **Jose Manuel Pose-Rodríguez:** Contributed to the protocol development and results interpretation. All authors discussed the evolution and commented on the manuscript at all stages.

Copyright © 2025 by the Editorial Council of *The Journal of Prosthetic Dentistry*. All rights are reserved, including those for text and data mining, AI training, and similar technologies.
<https://doi.org/10.1016/j.prosdent.2025.03.033>